Elk-3 is a KLF4-regulated gene that modulates the phagocytosis of bacteria by macrophages

Konstantin Tsoyi,* Adriana M. Geldart,[†,‡] Helen Christou,[†,‡] Xiaoli Liu,*[,†] Su Wol Chung,*[,§] and Mark A. Perrella*[,†,1]

*Division of Pulmonary and Critical Care Medicine, Department of Medicine, and [†]Department of Pediatric Newborn Medicine, Brigham and Women's Hospital and Harvard Medical School, Boston, Massachusetts, USA; [‡]Division of Newborn Medicine, Boston Children's Hospital and Harvard Medical School, Boston, Massachusetts, USA; and [§]School of Biological Sciences, University of Ulsan, South Korea

ABSTRACT

ETS family proteins play a role in immune responses. A unique member of this family, Elk-3, is a transcriptional repressor that regulates the expression of HO-1. Elk-3 is very sensitive to the effects of inflammatory mediators and is down-regulated by bacterial endotoxin (LPS). In the present study, exposure of mouse macrophages to *Escherichia coli* LPS resulted in decreased, full-length, and splice-variant isoforms of Elk-3. We isolated the Elk-3 promoter and demonstrated that LPS also decreased promoter activity. The Elk-3 promoter contains GC-rich regions that are putative binding sites for zinc-finger transcription factors, such as Sp1 and KLFs. Mutation of the GC-rich region from bp –613 to –603 blunted LPS-induced down-regulation of the Elk-3 promoter. Similar to the LPS response, coexpression of KLF4 led to repression of Elk-3 promoter activity, whereas coexpression of Sp1 increased activity. ChIP assays revealed that KLF4 binding to the Elk-3 promoter was increased by LPS exposure, and Sp1 binding was decreased. Thus, down-regulation of Elk-3 by bacterial LPS is regulated, in part, by the transcriptional repressor KLF4. Overexpression of Elk-3, in the presence of *E. coli* bacteria, resulted in decreased macrophage phagocytosis. To determine whether limited expression of HO-1 may contribute to this response, we exposed HO-1-deficient bone marrow-derived macrophages to *E. coli* and found a comparable reduction in bacterial phagocytosis. These data suggest that down-regulation of Elk-3 and the subsequent induction of HO-1 are important for macrophage function during the inflammatory response to infection. *J. Leukoc. Biol.* **97:** 171–180; 2015.

INTRODUCTION

ETS proteins encompass one of the largest families of transcription factors, with the prototype member, Ets-1 [1, 2]. Members of the ETS family of proteins regulate many important biologic processes in both normal and tumor cells, including the regulation of immune cell function [3, 4]. ETS family members retain a highly conserved 85 aa motif, designated as the Ets domain; recognize a core GGAA/T sequence, referred to as the EBS; and function as activators or repressors of gene transcription [2].

ETS transcription factors are divided into several subfamilies, based on homology within their Ets domains. The ELK subfamily contains the Ets domain at the N-terminus and a B-box domain that allows for the formation of a ternary complex with a serum response factor dimer, referred to as ternary complex factors [5]. One unique member of the ELK subfamily is Elk-3 (Net/E26 transformation-specific-related protein/serum response factor 2) [5, 6]. It has been shown that Elk-3 is a repressor of transcription [7], and this inhibitory effect on gene expression occurs through the NID [8] and the C-terminal-binding protein-interaction domain [9]. In addition to full-length Elk-3, there are alternatively spliced isoforms, Elk-3b and Elk-3c, that maintain the NID [10] and a more recently identified Elk-3d that lacks both inhibitor domains [11]. Interestingly, in the absence of inhibitor domains, the Elk-3d isoform is capable of activating gene transcription through EBS [11].

We have demonstrated previously that ETS transcription factors can activate or repress genes that are regulated by bacterial endotoxin (LPS) or peptidoglycan [12–16]. One such

1. Correspondence: Brigham and Women's Hospital,75 Francis Street, Boston, MA 02115, USA. E-mail: mperrella@rics.bwh.harvard.edu

gene is HO-1, a cytoprotective molecule that is transcriptionally induced during exposure to a number of pathophysiologic stimuli, including proinflammatory mediators [14, 16–18]. HO-1 and its products of heme catabolism, carbon monoxide, and bilirubin have anti-inflammatory and antioxidant properties [19–22], and mice deficient in HO-1 experience increased mortality, oxidative stress, and end-organ damage when exposed to bacterial endotoxin [23]. Thus, induction of HO-1 is important during endotoxemia and also sepsis [24, 25].

Whereas Ets-1, Ets-2, and Elk-1 have been shown to be positive transactivators of the HO-1 gene [14, 16], Elk-3 is a transcriptional repressor of HO-1 [13]. We have shown previously that in macrophages, the binding of Elk-3 to the HO-1 promoter helps to keep its activity at a lower level under basal conditions. However, when cells are exposed to an inflammatory stimulus, such as LPS, Elk-3 expression is rapidly down-regulated, releasing its repressive effects on promoter activity and allowing other members of the ETS family to increase transcriptional activity and HO-1 expression [13]. Thus, beyond positive transactivators, we believe the down-regulation of the transcriptional repressor Elk-3 during an inflammatory stimulus is critical for the tight control of gene expression. Beyond bacterial LPS, other stimuli promoting an inflammatory response, such as hypoxia [26], have also been shown to decrease Elk-3 expression [27, 28]. In the setting of HO-1 deficiency, these inflammatory stimuli are detrimental [23, 29], demonstrating the importance of HO-1 induction to compensate the inflammatory response. Whereas it has been shown that down-regulation of Elk-3 and removal of its repressive actions are able to enhance the expression of genes under inflammatory conditions (such as HO-1), little is known about regulation of the Elk-3 gene itself or the transcription factors that coordinate this response. Thus, the goal of this study was to elucidate the regulation of the Elk-3 gene by an inflammatory stimulus and to understand further the biologic consequences of Elk-3 down-regulation in macrophages.

MATERIALS AND METHODS

Cell culture

Murine macrophages (RAW 264.7) were grown according to the recommendations of the American Type Culture Collection (Manassas, VA, USA), as described previously [30]. Primary bone marrow-derived macrophages were also isolated and cultured as described previously [31]. In brief, bone marrow was flushed from femurs and tibias of WT and HO-1 KO mice by use of PBS. Cells were plated on sterile Petri dishes and incubated for 7 days in DMEM containing 10% (vol/vol) heat-inactivated FBS, penicillin, and streptomycin and 25% (vol/vol) conditioned medium from L929 mouse fibroblasts. LPS from *E. coli* (serotype O26:B6) was purchased from Sigma-Aldrich (St. Louis, MO, USA).

RNA extraction and qRT-PCR

Total RNA was extracted from RAW 264.7 cells by TRIzol reagent, according to the manufacturer's instructions (Life Technologies, Carlsbad, CA, USA). qRT-PCR, with SYBR Green Master Mix (Bio-Rad Laboratories, Hercules, CA, USA), was performed by use of the StepOnePlus Real-Time PCR System (Applied Biosystems, Foster City, CA, USA). The relative quantity of target mRNA was calculated by use of the CT method, or $2^{-\Delta\Delta CT}$, as described [32], and normalized by use of β-actin as an endogenous control (Sequence Detection System software, version 1.7; Applied Biosystems). To discriminate among Elk-3 mRNA isoforms, we used a common reverse primer 5′-TGT GTT CGG CCC TTG CA-3′ and isoform-specific forward primers to detect Elk-3/Elk-3b (5′-CCT TCT TCA CCG CAC AGA CA-3′), Elk-3c (5′-TCA GGA CTG TGA TCA GAC ACC AA-3′), and Elk-3d (5′-CTG AGA TAC TAT TAC GAC AAG ACA CCA A-3′) [11].

Plasmid constructs and gene-silencing reagents

The mouse Elk-3 transcription start site (chromosome 10: 93311159, reverse strand) was identified by use of the University of California at Santa Cruz (Santa Cruz, CA, USA) genome browser. The Elk-3 gene, including the promoter region, was isolated from a bacteriophage artificial chromosome library, derived from mouse spleen genomic DNA (RPCI22.HYB; BACPAC Resources Center, Oakland, CA, USA). Forward (5′-GGG AGT CTT CTT GGG GAG A-3′) and reverse (5′-CGA AAA CTA CTG GTC AGA AAG-3′) primers were used to amplify region 93310772-93311934 of chromosome 10 and designated this promoter region as Elk-3 (–775/+387) by iProof High-Fidelity Master Mix (Bio-Rad Laboratories). Deletion constructs Elk-3 (–463/+387), Elk-3 (–163/+387), and Elk-3 (+187/+387) were generated by use of common forward (5′-GGG AGT CTT CTT GGG GAG A-3′) and different reverse (5′-CCC AAA AGA GGA TCC CAA CTC-3′, 5′-CCA TTA GCA GGG CAC GAA C-3′, and 5′-CCA ACT CCT GCT CTC ACA ACA-3′) primers, respectively. PCR products were verified by sequencing and cloned into the pGL3-basic vector (Promega, Madison, WI, USA) by use of the TA Cloning Kit (Invitrogen, Carlsbad, CA, USA). For the Elk-3 silencing experiments, Elk-3 target sequence CGAAGCCATATTTAGACAATA, or a Scr sequence, was cloned into the pMSVC vector (Open Biosystems, GE Dharmacon, Lafayette, CO, USA), and retroviral particles were made in the EcoPack 2-293 cell line (Clontech Laboratories, Mountain View, CA, USA). The RAW 264.7 cells were infected with the retroviral particles, and stably transfected cells were then selected by use of puromycin [33, 34]. Elk-3 shRNA and Scr shRNA cells were used for phagocytosis assays. For the KLF4 silencing experiments, the pLKO.1 plasmid, carrying the KLF4 target sequence CTCTCTCACATGAAGCGACTT (consortium number TRCN0000095370), or pLKO.1, carrying a Scr sequence, was purchased from Sigma-Aldrich. Lentiviral particles were generated by use of commercially available packaging mix, provided by Sigma-Aldrich (catalog number SHP001) in human embryonic kidney 293 T cells, according to the manufacturer's instructions. The RAW 264.7 cells were infected with the lentiviral particles, and stably infected cells were selected by use of puromycin (10 μg/ml). KLF4 shRNA and Scr shRNA cells were used for evaluation of the Elk-3 promoter. For cells that were silenced for Elk-3 or KLF4, the reduced level of target gene expression was confirmed by qRT-PCR (Supplemental Fig. 1A and B, respectively). Expression plasmids pcDNA3.1-KLF4 or pcDNA3.1-Sp1 were cotransfected by use of FuGENE 6 into RAW 264.7 cells for Elk-3 promoter analysis studies, whereas pCI-Elk-3 or pFLAG-CMV-5a-HO-1 were transiently transfected the cells for assessment of phagocytosis. For the generation of RAW 264.7 cells overexpressing Elk-3 for the confocal microscopy experiments, the coding region of Elk-3 was amplified from plasmid pCI-Elk-3 by use of forward (5′-ATG GAG AGT GCA ATC ACG CTG TG-3′) and reverse (5′-TCC CCC AGC TCT CAG AAA TCC-3′) primers. The PCR product was then cloned into pCMV6-entry plasmid, containing a neomycin-resistant gene (OriGene Technologies, Rockville, MD, USA). Transfections of RAW 264.7 cells with pCMV6-Elk-3 or the vector alone (pCMV6) were performed by use of FuGENE 6, and stably transfected cells were selected by use of G418 (2 mg/ml) for 7 days. pCMV6-Elk-3 or vector-alone cells were used for phagocytosis assays, followed by confocal microscopy.

Site-directed mutagenesis and internal deletion constructs

The mGC-rich binding site at −613 bp of the Elk-3 promoter was generated by site-directed mutagenesis of construct Elk-3 (−775/+387) by use of the Pfu polymerase (Stratagene, Agilent Technologies, Santa Clara, CA, USA). The mGC-rich binding site, from bp −613 to −603, was generated by substituting sequence mTCCCaaCCCC for WT sequence TCCCcgCCCC in the forward (5′-TGG ACT CCC AAC CCC TGA GGA CAA TGG CCA GGA TCT GAT-3′)

and reverse (5′-TTG TCC TCA <u>GGG GTT GGG A</u>GT CCA GTC TTG AAA CCA CA-3′) PCR primers. Mutated sequences are underlined. The PCR products were digested with *Dpn*I, and the undigested plasmids were transformed into XL2-Blue bacteria (Stratagene, Agilent Technologies). Internal deletion of a GC-rich region in construct Elk-3 (−775/+387), encompassing bp −19 to +112, was performed by use of forward (5′-TGT AAA CAG GCT TTG CTT CCT GCT CGG-3′) and reverse (5′-CCG AGC AGG AAG CAA AGC CTG TTT ACA-3′) PCR primers. After the amplification reaction, PCR products were digested with *Dpn*I, and the undigested plasmids were transformed into XL2-Blue bacteria (Stratagene, Agilent Technologies), as described previously [16]. For these mutated constructs, sequencing was performed to verify the incorporation of the site mutation or internal deletion.

Luciferase assays

Transient transfection assays in RAW 264.7 cells were performed by use of FuGENE 6 transfection reagent (Roche Applied Science, Indianapolis, IN, USA), as described previously [13, 16]. For promoter analyses, Elk-3 promoter-reporter constructs (500 ng/well) and a β-galactosidase expression plasmid (250 ng/well) to correct for transfection efficiency were cotransfected into murine macrophages. When assessing the response to transcription factors, Elk-3 promoter-reporter constructs (350 ng/well) and a β-galactosidase expression plasmid (250 ng/well) were cotransfected in conjunction with KLF4 or Sp1 expression plasmids (400 ng/well). For the luciferase assays, 3×10^5 cells/well were plated in triplicate on 6-well plates and incubated for 24 h. Twenty-four hours later, vehicle or LPS (100 ng/ml) was administered. The cells were harvested for luciferase activity by use of the Luciferase Assay System (Promega), 6 h after treatment. Luciferase activity was measured in a Wallace Victor3 1420 multilabel counter (PerkinElmer, Waltham, MA, USA). β-Galactosidase activity was measured by use of the mammalian β-Galactosidase Assay Kit (Thermo Fisher Scientific, Waltham, MA, USA). Transfection efficiency was 24 ± 3.2% for the transient assays.

ChIP assay

The ChIP assay was performed by use of an enzymatic Chromatin IP kit from Cell Signaling Technology (catalog number 9002), according to the manufacturer's instructions. In brief, RAW 264.7 cells were exposed to vehicle or LPS for 6 h and then fixed in 1% formaldehyde for 10 min at room temperature. Cross-linking was stopped by adding glycine. DNA was digested by use of micrococcal nuclease to the length of ~150-900 bp. Before incubation with antibodies, 10 μl of input control solution was taken from each sample. The remaining chromatin solution was incubated with 10 μg anti-KLF4 or anti-Sp1 antibody at 4°C overnight (Santa Cruz Biotechnology, Santa Cruz, CA, USA). Immune complexes were precipitated, washed, and eluted as recommended. DNA-protein cross-links were reversed by heating at 65°C for 2 h, and 10 μl of each sample was used as a template for qRT-PCR. Elk-3 oligonucleotide sequences for PCR primers were forward 5′-GGC TTT AGA CAG GCA CTG CTT-3′ and reverse 5′-CTC CTG CAT CCT CCG AGC AAT-3′. This primer set encompasses the Elk-3 promoter segment from nucleotide −671 to −530. The relative quantity of target Elk-3 promoter was calculated by by use of the *C*T method (Sequence Detection System software, version 1.7; Applied Biosystems), or $2^{-\Delta\Delta CT}$, as described [32]. The $2^{-\Delta\Delta CT}$ from immunoprecipitation samples by use of the anti KLF4 or anti-Sp1 antibodies was normalized with the $2^{-\Delta\Delta CT}$ from the input control samples and graphed as a percentage of the samples not exposed to LPS.

Western blot analysis

Whole cell lysates were harvested from cells, and the concentration of each sample was determined by use of a bicinchoninic acid protein assay kit (Pierce, Thermo Fisher Scientific, Rockford, IL, USA). Western blotting for HO-1 and β-actin were performed as described previously [25] by use of antibodies from Santa Cruz Biotechnology. To detect Elk-3, the total protein lysate was electrophoresed on a polyacrylamide gel, which was transferred to PVDF membranes by use of semidry electrophoretic transfer. The PVDF membranes were then blocked for 2 h at room temperature in 5% BSA. The

membranes were washed in TBST buffer for 2 h, periodically changing TBST buffer every 15 min. After washing, the membranes were incubated overnight at 4°C with a rabbit polyclonal antibody against Elk-3 (Abcam, Cambridge, United Kingdom), diluted 1:500 in a solution containing 5% BSA. The next day, the membranes were washed and then incubated with a HRP-conjugated secondary antibody (Santa Cruz Technology) at room temperature for 1 h. The signals were detected by ECL and quantitated by use of the ChemiDoc XRS+ System (Bio-Rad Laboratories).

Phagocytosis assay

Mouse macrophages (RAW 264.7 or primary bone marrow-derived macrophages) were plated and incubated overnight in complete media. Then, GFP-labeled *E. coli* (strain MMB1287) was added at 10 MOI/cell. To examine the extent of phagocytosis, cells were harvested after 2 h (except for the Elk-3 shRNA experiments, in which phagocytosis was performed at 15 min before Elk-3 down-regulation by bacteria), stained with 0.2% Trypan blue for 1 min to quench extracellular fluorescence, washed, and incubated with F4/80-allophycocyanin-conjugated antibody (BioLegend, San Diego, CA, USA). Following staining, cells were fixed (BD Cytofix/Cytoperm; BD Biosciences, San Jose, CA, USA), and flow cytometry was performed by use of a BD FACSCanto II (BD Biosciences). Gating for the GFP and F4/80 channels is presented in Supplemental Fig. 2. At least 10,000 events were collected, data were analyzed by use of FlowJo software, and changes were documented as MFI [35]. For the phagocytosis assays, in which confocal imaging was performed, GFP-labeled *E. coli* was added at 100 MOI/RAW 264.7 cell. After 2 h, the cells were washed and stained with 0.2% Trypan blue for 1 min to quench extracellular fluorescence, washed, and then fixed with 4% paraformaldehyde for 10 min. The cell membranes were next stained with PKH26 (400 μM for 5 min; Sigma-Aldrich), and then nuclei were stained with DAPI (Invitrogen). The cells were next imaged by use of confocal microscopy (FluoView FV1000 unit with IX81 inverted microscope; ×600; Olympus, Center Valley, PA, USA): GFP-labeled bacteria (green), cell membrane stained with PKH26 (red), and nuclei stained with DAPI (blue). To quantitate phagocytosis, the percentage of cells that had phagocytized bacteria was assessed by fluorescent microscopy by use of 6 random images of each group and performed in two separate experiments.

Statistics

Data are presented as mean ± SEM. For comparisons between two groups, we used Student's two-tailed, unpaired *t*-test. One-way analysis of variance, followed by Newman-Keuls or Tukey's post-test analysis, was used for comparisons of more than two groups. The numbers of samples/group (*n*) or the numbers of experiments are specified in the figure legends. Statistical significance is accepted at $P < 0.05$.

RESULTS

Elk-3 and its isoforms are down-regulated by LPS in macrophages

The Elk-3 gene is expressed not only as a full-length (whole) form but also as alternatively spliced isoforms, as shown in **Fig. 1A** [10, 11]. Thus, we were interested to clarify which of the Elk-3 isoforms are expressed in macrophages. Elk-3 whole/b was the predominant isoform expressed in macrophages, whereas, isoforms Elk-3c and Elk-3d were expressed at very low mRNA levels. LPS stimulation greatly suppressed the mRNA levels of Elk-3 whole/b in a dose- and time-dependent fashion (Fig. 1B and C). Interestingly, LPS also down-regulated Elk-3c and Elk-3d mRNA levels (Supplemental Fig. 3A and B). Based on these data, we believe that full-length Elk-3 and its alternatively spliced isoforms are regulated in a comparable manner by LPS stimulation in macrophages.
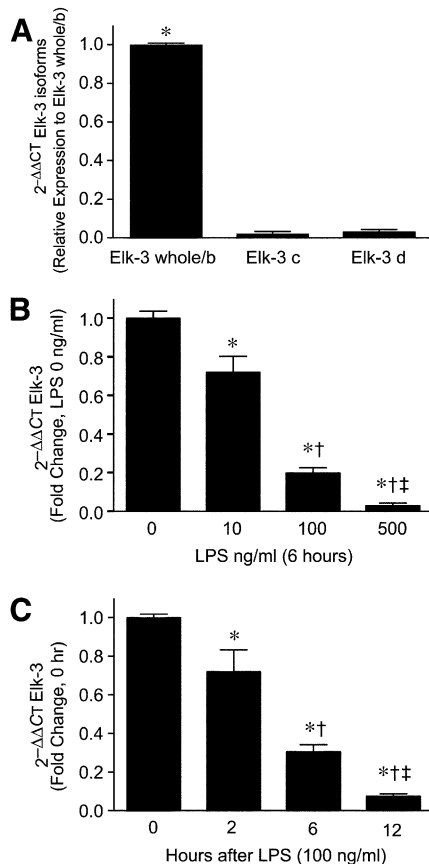
Figure 1. Elk-3 is down-regulated by LPS in a dose- and time-dependent manner in macrophages. (A) Total RNA was isolated from RAW 264.7 cells, and levels of Elk-3 isoforms were measured by qRT-PCR by use of the comparative CT method ($2^{-\Delta\Delta CT}$; also used for B and C). Data are presented as mean $\pm$ SEM; $n = 4$/group, with testing by one-way ANOVA (*$P < 0.0001$, significant comparison vs. Elk-3c and Elk-3d). (B) Cells were exposed to LPS at concentrations of 10, 100, and 500 ng/ml for 6 h. After incubation, total RNA was extracted from cells, and Elk-3 levels were measured by qRT-PCR. The data are presented as mean $\pm$ SEM, $n = 4$/group, with testing by one-way ANOVA ($P < 0.0001$; significant comparisons: * vs. LPS 0 ng/ml; † vs. LPS 10 ng/ml; and ‡ vs. LPS 100 ng/ml). (C) Cells were exposed to LPS (100 ng/ml) for 0, 2, 6, and 12 h. After exposure, total RNA was isolated, and Elk-3 levels were measured by qRT-PCR. The data are presented as mean $\pm$ SEM, $n = 4$/group, with testing by one-way ANOVA ($P < 0.0001$; significant comparisons: * vs. 0 h; † vs. 2 h; and ‡ vs. 6 h after LPS).

LPS down-regulates Elk-3 promoter activity in macrophages

As a result of this similar suppression of Elk-3 and its isoforms at the mRNA level, we hypothesized that the regulation of the Elk-3 gene by LPS may occur at the level of gene transcription. To test this hypothesis, we cloned the Elk-3 promoter (−775/+387) into a luciferase reporter plasmid (pGL3) and transfected the plasmid into macrophages to assess promoter regulation by LPS. As shown in **Fig. 2A** and **B**, LPS treatment significantly decreased Elk-3 promoter activity in a dose- and time-dependent manner. To identify LPS-responsive elements, Elk-3 promoter deletion plasmids were constructed, as shown in **Fig. 3** (top). LPS decreased promoter activity of Elk-3 (−775/+387) by 53%.
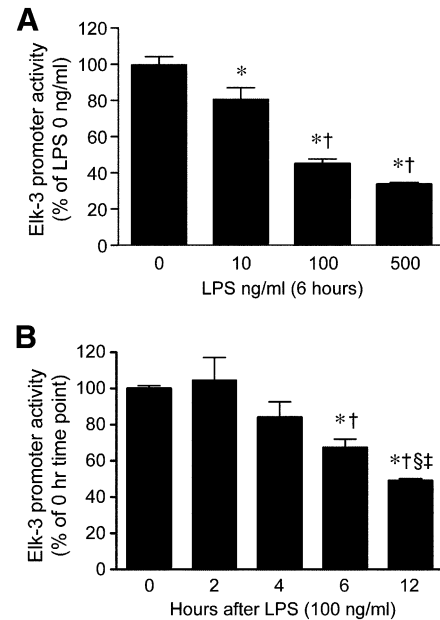

Figure 2. LPS down-regulates Elk-3 promoter activity in macrophages. RAW 264.7 cells were transiently transfected with Elk-3 promoter plasmid (500 ng/well) and an expression plasmid for β-galactosidase (250 ng/well) to correct for transfection efficiency. (A) Cells were allowed to recover overnight, and then the cells were exposed to LPS (10, 100, 500 ng/ml) for 6 h before harvest. Luciferase activity of each group is presented as mean $\pm$ SEM, $n = 9$/group (from 3 independent experiments), with testing by one-way ANOVA ($P < 0.0001$; significant comparisons: * vs. LPS 0 ng/ml and † vs. LPS 10 ng/ml). (B) Cells were exposed to LPS (100 ng/ml) for 0, 2, 4, 6, and 12 h before harvest. Luciferase activity of each group is presented as mean $\pm$ SEM, $n = 9$/group (from 3 independent experiments), with testing by one-way ANOVA ($P < 0.0013$; significant comparisons: * vs. 0 h; † vs. 2 h; ‡ vs. 6 h; and § vs. 4 h after LPS).

However, this degree of suppression in promoter activity by LPS was blunted in deletion constructs Elk-3 (−463/+387) and Elk-3 (+187/+387), 32% and 14% decreases, respectively (Fig. 3). These data suggest that regions −775 to −463 and −163 to +187, may be important for the LPS-induced decrease in Elk-3 transactivation. Interestingly, both of these LPS-responsive regions of the Elk-3 promoter contain prominent GC-rich domains (−613 to −603 and −19 to +112). To clarify the importance of these GC-rich regions, mutations of −613 to −603 and/or deletion of −19 to +112 of the Elk-3 promoter were performed. As demonstrated in **Fig. 4**, the LPS suppression was significantly attenuated in the Elk-3 construct, with mutation in the GC-rich region (mGC-rich), beginning at −613. However, the construct with deletion of the GC-rich region from −19 to +112 did not attenuate LPS suppression nor did a construct with disruption of both GC-rich regions further blunt the LPS-induced reduction in promoter activity compared with the construct containing the mGC-rich region (beginning at −613). These data demonstrate that the GC-rich region from −613 to −603 is vital for the LPS inhibitory effect on Elk-3 promoter activity in macrophages.

We also assessed the effects of the Elk-3 promoter deletion constructs on basal promoter activity, independent of LPS. As seen in Supplemental Fig. 4A, deletion from −775 to −463
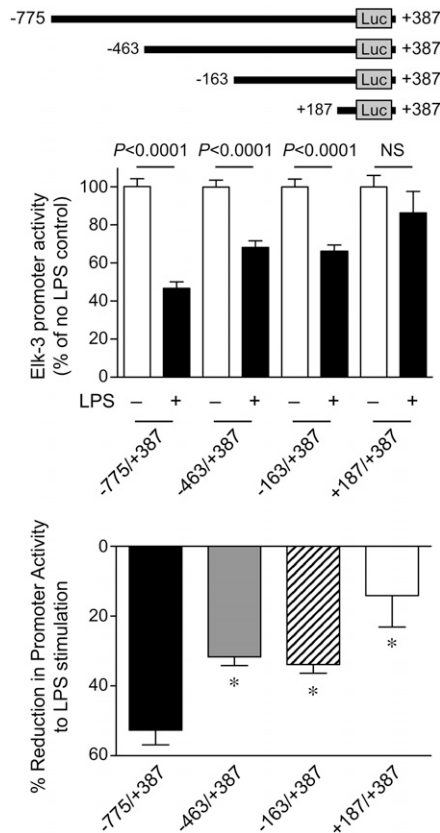
Figure 3. Elk-3 promoter contains LPS-responsive region(s) downstream of –775 bp and –163 bp. Elk-3 promoter deletion constructs Elk-3 (–775/+387), Elk-3 (–463/+387), Elk-3 (–163/+387), and Elk-3 (+187/+387) were generated (top). RAW 264.7 cells were transiently transfected with these promoter deletion plasmids, along with an expression plasmid for β-galactosidase to correct for transfection efficiency. Cells were allowed to recover overnight and were then exposed to LPS (100 ng/ml) or vehicle for 6 h. (Middle) Luciferase (LUC) activity as mean ± SEM in the presence (+) or absence (–) of LPS, $n = 9$/group (from 3 independent experiments), comparing LPS-exposed cells with its control in each group by unpaired *t*-test. *P* values are provided above the bars or no significance (NS). (Bottom) Luciferase activity of each group is presented as a percentage change relative to cells not receiving LPS. The data are presented as mean ± SEM, $n = 9$/group (from 3 independent experiments), with testing by one-way ANOVA (*$P < 0.002$, significant comparisons vs. –775/+387).

resulted in an increase in Elk-3 promoter activity, which was increased further by deletion of the promoter to –163. In contrast, deletion of the Elk-3 promoter to +187 resulted in a marked decrease in promoter activity. These data demonstrate that repressor regions for the basal promoter exist between –775 and –163 of the Elk-3 5′-flanking sequence. Once the deletion goes beyond the transcription start site, the overall basal promoter activity decreases significantly (Supplemental Fig. 4A). To determine whether the GC-rich regions of the Elk-3 promoter are responsible for the changes in basal promoter activity, we assessed the promoter constructs with mutations in region –613 to –603 or deletion of the GC-rich region from –19 to +112. In both circumstances, alterations in the GC-rich regions of the Elk-3 5′-flanking sequence did not significantly change basal promoter activity (Supplemental Fig. 4B). These data
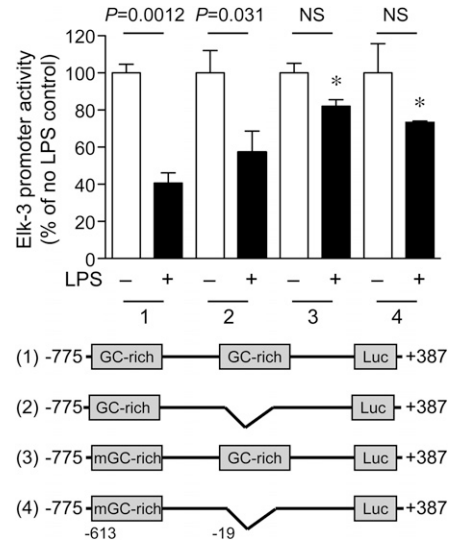

Figure 4. GC-rich binding site at −613 to -603 bp of Elk-3 promoter is important for LPS-induced down-regulation of Elk-3 promoter. RAW 264.7 cells were transiently transfected with (1) WT promoter construct Elk-3 (−775/+387); (2) Elk-3 (−775/+387), with GC-rich region −19 to +112 bp deleted; (3) Elk-3 (−775/+387), with mutation of GC-rich region−613 to −603 bp; or (4) both GC-rich regions disrupted. Along with the promoter constructs, an expression plasmid for β-galactosidase was transfected to correct for transfection efficiency. The cells were allowed to recover overnight and were then exposed to LPS (100 ng/ml) or vehicle for 6 h. Luciferase activity for each group is presented as mean ± SEM in the presence (+) or absence (–) of LPS, $n = 9$/group (from 3 independent experiments), comparing LPS-exposed cells with its control in each group by unpaired *t*-test. *P* values are provided above the bars or no significance. Comparisons between groups are made by one-way ANOVA ($P < 0.0001$). Significant comparisons; * versus WT Elk-3 (−775/+387) + LPS.

demonstrate that the GC-rich regions are predominantly regulating the response of the Elk-3 promoter to LPS.

KLF4 and Sp1 transcription factors regulate the Elk-3 promoter

GC-rich motifs are putative binding sites for zinc-finger transcription factors, such as Sp1 and KLF4 [36, 37]. Thus, we wanted to know whether Sp1 and KLF4 might play a role in Elk-3 promoter regulation by LPS. As shown in **Fig. 5A**, overexpression of KLF4 significantly reduced Elk-3 promoter activity in macrophages, mimicking the LPS effect, whereas overexpression of Sp1 increased Elk-3 promoter activity. ChIP assays were next performed in macrophages to assess in vivo binding of transcription factors to region –613 to –603 of the Elk-3 promoter in the presence or absence of LPS. ChIP for histone H3 was used as a positive control for this assay (Fig. 5B). Figure 5C demonstrates that LPS stimulation of macrophages enhanced KLF4 binding in region –613 to –603 of the Elk-3 promoter, whereas Sp1 binding in this region decreased. Thus, a switch in binding of transcription factors in this GC-rich region after exposure to LPS, from Sp1 to KLF4, contributes to the suppression of Elk-3 by LPS. To demonstrate the importance of KLF4 in the regulation of Elk-3 by LPS, KLF4 was silenced in macrophages by use of shRNA compared with Scr (control) shRNA. In cells silenced for KLF4, the reduction in Elk-3
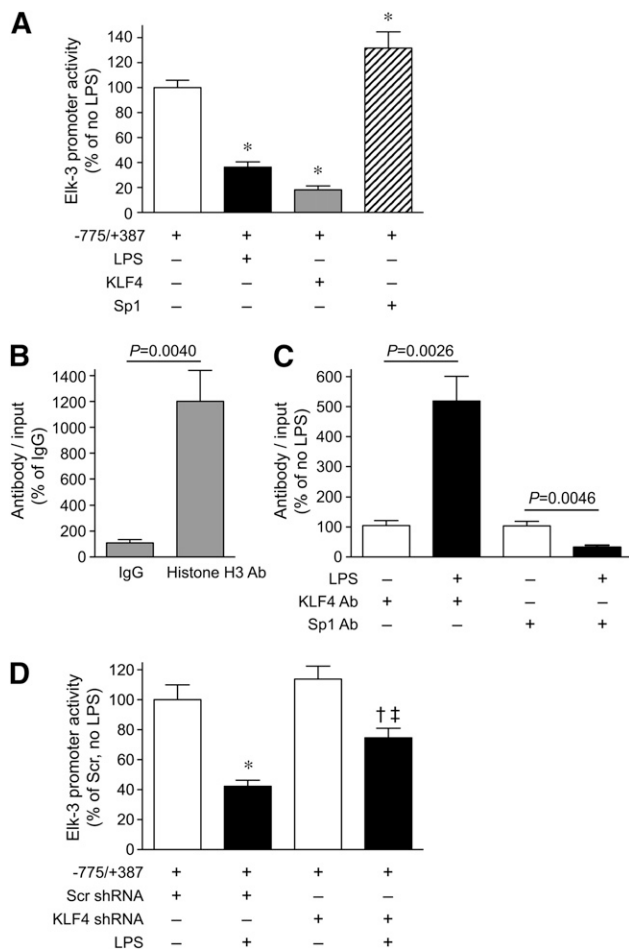
A

B

C

D

Figure 5. KLF4 is an important transcription factor for repression of the Elk-3 promoter by LPS in macrophages. (A) RAW 264.7 cells were transiently cotransfected with Elk-3 promoter (−775/+387) and either an empty vector (−) or expression plasmids for KLF4 or Sp1 (+). The cells were also transfected with an expression plasmid for β-galactosidase to correct for transfection efficiency. Cells were allowed to recover overnight and were then exposed to LPS (+; 100 ng/ml) or vehicle (−) for 6 h. Luciferase activity for each group is presented as a percentage change relative to untreated cells, n = 6/group (from 2 independent experiments) and comparisons made by one-way ANOVA (*$P < 0.0001$, significant comparisons vs. untreated cells). RAW 264.7 cells were either not stimulated (B) or exposed to LPS (+; 100 ng/ml) or vehicle (−) for 6 h (C). The cells were next fixed with 1% formaldehyde for 10 min and then harvested for ChIP assay, as described in Materials and Methods. (B) The untreated samples were incubated with IgG (negative control) or histone H3 antibody (positive control). (C) The samples were incubated with an antibody to KLF4 or Sp1. Binding of protein to DNA was assessed by qRT-PCR, by use of the CT method ($2^{-\Delta\Delta CT}$), normalized with the $2^{-\Delta\Delta CT}$ from the input control samples, and graphed as a percentage of the samples not exposed to LPS. The data are presented as mean ± SEM, n = 4 (from two independent experiments), with testing by unpaired t-test in B and C. P values are provided above the bars. (D) RAW 264.7 cells silenced for KLF4 (KLF4 shRNA) or a Scr control (Scr shRNA) were transiently cotransfected with Elk-3 promoter (−775/+387), along with an expression plasmid for β-galactosidase, to correct for transfection efficiency. The cells were then exposed to LPS (+; 100 ng/ml) or vehicle (−) for 6 h. Luciferase activity for each group is presented as a percentage change relative to Scr shRNA – LPS, n = 9/group (from 3 independent experiments) and comparisons made by one-way ANOVA ($P < 0.0001$; significant comparisons: * vs. Scr shRNA – LPS; † vs. KLF4 shRNA – LPS; and ‡ vs. Scr shRNA + LPS).

promoter activity by LPS was significantly less than the reduction in promoter activity in cells receiving Scr shRNA (Fig. 5D). These data confirm that KLF4 contributes to the repression of the Elk-3 promoter in the presence of LPS. Interestingly, the silencing of KLF4 did not increase Elk-3 promoter activity in the absence of LPS, and this is consistent with the fact that under basal conditions, Sp1 and not KLF4 is binding to the Elk-3 promoter (Fig. 5C).

Elk-3 overexpression decreases *E. coli* phagocytosis and inhibits HO-1 expression

We next wanted to determine whether Elk-3 modulates macrophage phagocytic activity, as phagocytosis of microbial pathogens by innate immune cells is a critical component of the host response to infection [38]. As shown in **Fig. 6A**, over-expression of Elk-3 is able to maintain the expression level of Elk-3 at basal levels when exposed to *E. coli* LPS. In the presence of live bacteria, macrophages overexpressing Elk-3 showed a 3-fold reduction in the percentage of cells phagocytizing bacteria by confocal microscopy (Fig. 6B), and fewer bacteria phagocytized per cell compared with vector control cells. These data were confirmed by use of flow cytometry and demonstrated that overexpression of Elk-3 led to a 46% decrease in phagocytosis of GFP-labeled *E. coli*, as assessed by MFI (Fig. 6C). In contrast, the silencing of Elk-3 in macrophages by use of shRNA led to an acute increase in the phagocytosis of *E. coli* compared with a Scr (control) shRNA (Fig. 6D), as assessed by flow cytometry.

Finally, overexpression of Elk-3 attenuated the level of HO-1 expression during LPS exposure (**Fig. 7A**). To determine whether a lower expression level of HO-1 may contribute to the decrease in macrophage phagocytosis, we harvested bone marrow-derived macrophages from HO-1-deficient mice and exposed the cells to *E. coli*. Figure 7B demonstrates that HO-1-deficient macrophages have reduced bacterial phagocyto-sis compared with WT macrophages. When performing the inverse experiment, overexpression of HO-1 in macrophages led to an increase in phagocytosis of *E. coli* compared with vector control cells (Fig. 7C). Taken together, these data suggest that Elk-3 is a negative regulator of bacterial phagocytosis and that the effect of Elk-3 levels on HO-1 expression may contribute to the phagocytic response.

DISCUSSION

Elk-3 is a transcriptional repressor in the ELK subfamily of ETS factors [5–7], and it is expressed in a full-length form or as alternatively spliced isoforms lacking regions or the entirety of exon 3 [11]. We [12, 13] and others [27, 28] have shown previously that Elk-3 is responsive to the effects of inflammatory stimuli, and in the present study, we demonstrate that full-length Elk-3 mRNA is the most predominate isoform in mouse macro-phages, and its message is down-regulated in a dose- and time-dependent manner by bacterial LPS (Fig. 1). Alternative spliced isoforms of Elk-3 are also decreased by LPS (Supplemental Fig. 3), suggesting a common manner of gene regulation. However, to date, the mechanism responsible for this down-regulation of Elk-3 has not been elucidated. The cloning of the Elk-3 5′-flanking sequence and subsequent promoter-reporter assays demonstrated
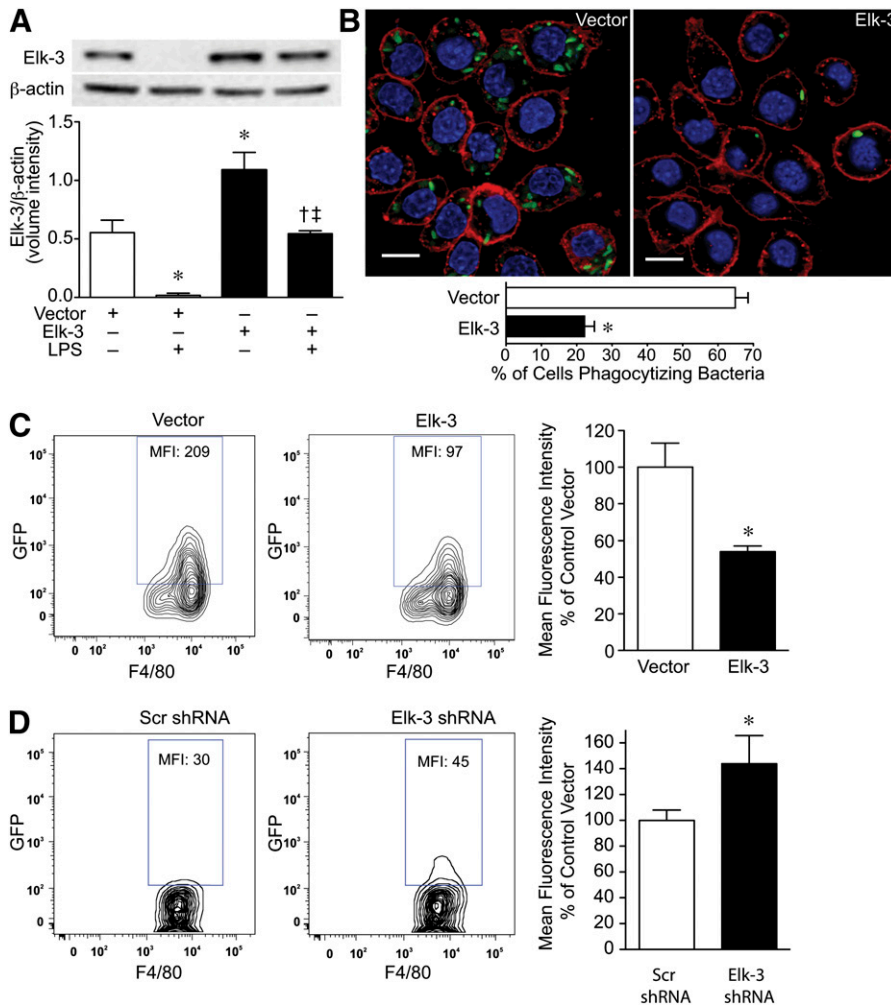
Figure 6. Overexpression of Elk-3 in macrophages decreases bacterial phagocytosis. (A) RAW 264.7 cells were transfected with pcDNA3.1 (control, empty vector) or pcDNA3.1-Elk-3 plasmid. The cells were allowed to recover overnight and were then exposed to *E. coli* LPS (+; 100 ng/ml) or vehicle (–) for 6 h. Total protein was then harvested from the cells for Western blot analyses. (Upper) Representative Western blots for Elk-3 and β-actin as a loading control. The blots were then quantitated for expression of Elk-3, corrected by β-actin expression, and plotted as a mean volume intensity ± SEM (lower). The data represent 3 independent experiments, with comparisons between groups made by one-way ANOVA ($P = 0.0003$; significance comparisons: * vs. vector control; † vs. vector control plus LPS; and ‡ vs. Elk-3 overexpression in the absence of LPS). (B) RAW 264.7 cells were stably transfected with control vector or Elk-3. GFP-labeled *E. coli* was added at 100 MOI/cell. After 2 h, the cells were washed and processed for phagocytosis, as described in Materials and Methods. The cells were next imaged by use of confocal microscopy (×600): GFP-labeled bacteria (green); cell membrane stained with PKH26 (red); and nuclei stained with DAPI (blue). The scale bars represent 10 μm. To quantitate phagocytosis, the percentage of cells that had phagocytized bacteria was assessed by fluorescent microscopy by use of 6 random images of each group and performed in two separate experiments. The data represent the percent of cells phagocytizing bacteria (2 independent experiments), with testing by unpaired *t*-test (*$P < 0.0001$, significance comparison vs. vector control). (C) RAW 264.7 cells were transfected with pCI (control, empty vector) or pCI-Elk-3 expression plasmid. Cells were allowed to recover overnight. The next day, GFP-labeled *E. coli* was added at 10 MOI/cell. After 2 h, cells were washed and processed for phagocytosis, as described in Materials and Methods. (Left and middle) Representative flow cytometry zebra plots for macrophages (F4/80+), transfected with vector control or Elk-3, which phagocytized GFP-labeled *E. coli*. Quantification is assessed by MFI. (Right) The data are presented as percentage MFI of vector control, *n* = 4 independent experiments, with testing by unpaired *t*-test (*$P = 0.0147$, significance comparison vs. vector control). (D) RAW 264.7 were silenced with Elk-3 shRNA or Scr shRNA as a control. GFP-labeled *E. coli* was added at 10 MOI/cell. After 15 min, cells were washed and processed for phagocytosis, as described in Materials and Methods. (Left and middle) Representative flow cytometry zebra plots for macrophages (F4/80+), transfected with Scr shRNA or Elk-3 shRNA, which phagocytized GFP-labeled *E. coli*. Quantification is assessed by MFI. (Right) The data are presented as percentage MFI of Scr shRNA, *n* = 6 (3 independent experiments), with testing by unpaired *t*-test (*$P = 0.045$, significance comparison vs. Scr shRNA).

that LPS is also able to down-regulate the Elk-3 promoter (Fig. 2). These data suggest that repression of transcription contributes to the down-regulation of Elk-3 mRNA by LPS.

Deletion analysis of the Elk-3 promoter revealed that regions between bp –775 and –463 and –163 and +187 contain LPS-induced repressor elements (Fig. 3). In reviewing these regions of the 5′-flanking sequence, each segment contained prominent GC-rich regions, starting at bp –613 and –19, respectively. Whereas deletion of region –19 to +112 had little effect on repression of the Elk-3 promoter by LPS, mutation of the GC-rich site between –613 and –603 significantly blunted LPS-induced repression (Fig. 4). These data suggest that transcription factors binding to GC-rich sequences may contribute to the down-regulation of Elk-3 by bacterial LPS.
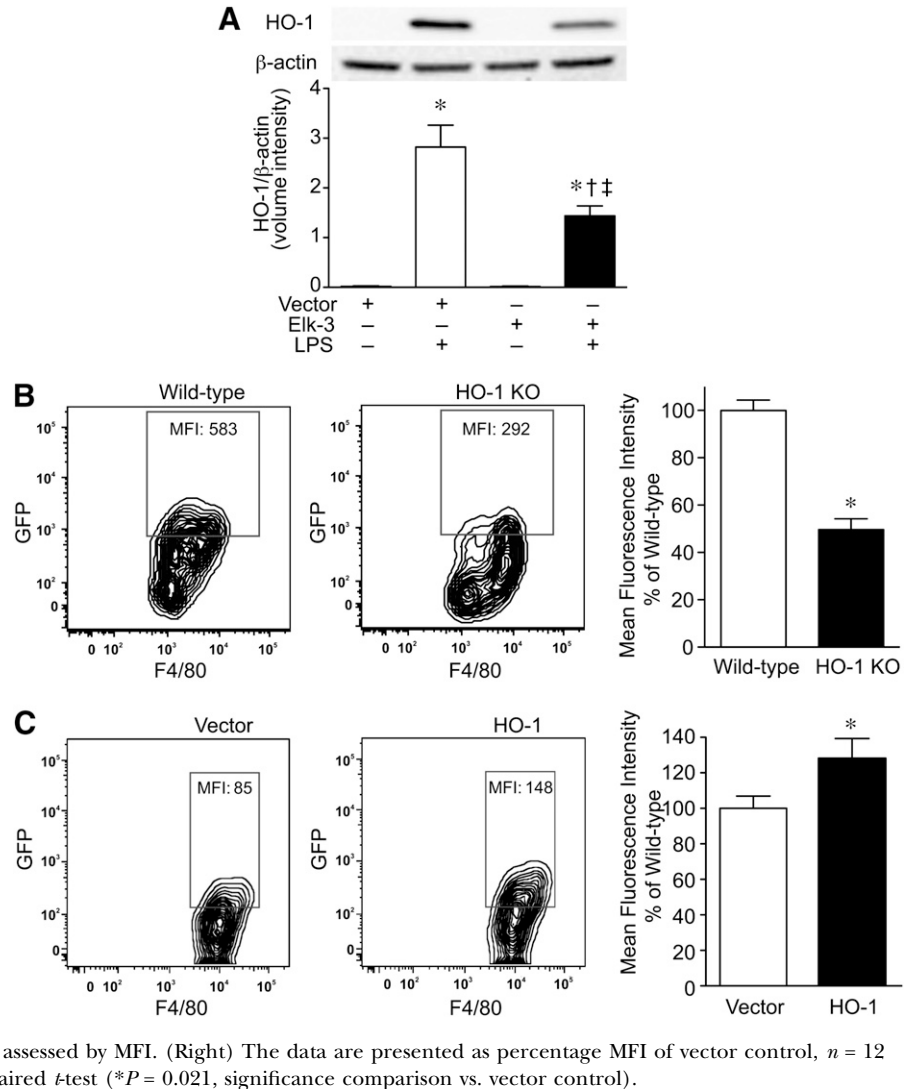
Sp1 is a well-characterized transcription factor that regulates numerous biologically important genes by binding to GC-rich

promoter elements via zinc-finger motifs [36, 37]. Additional Sp1-like proteins have also been characterized by the presence of conserved DNA-binding domains, comprising three Krüppel-like zinc fingers [36, 37]. Similar to Sp1, these KLFs bind GC-rich DNA elements and regulate gene transcription. However, whereas Sp1 is a transcriptional activator, the KLF proteins can function as activators or repressors of transcription, depending on the promoter to which they bind and the cellular environment [36]. In fact, it has been suggested that KLF proteins can inhibit promoter activity by competing with Sp1 at GC-rich binding sites [37, 39, 40].

We present data to demonstrate that KLF4, a KLF family member with repressor activity, contributes to the down-regulation of Elk-3 by LPS in mouse macrophages. Over-expression of KLF4 alone produced a decrease in Elk-3 promoter activity, comparable with the effect of LPS (Fig. 5A). As expected,

Figure 7. Deficiency of HO-1 in macrophages leads to decreased bacterial phagocytosis. (A) RAW 264.7 cells were transfected with pcDNA3.1 (control, empty vector) or pcDNA3.1-Elk-3 plasmid. The cells were allowed to recover overnight and were then exposed to *E. coli* LPS (+; 100 ng/ml) or vehicle (−) for 6 h. Total protein was then harvested from the cells for Western blot analyses. (Upper) Representative Western blots for HO-1 and β-actin as a loading control. The blots were then quantitated for expression of HO-1, corrected by β-actin expression, and plotted as a mean volume intensity ± SEM (lower). The data represent 3 independent experiments, with comparisons between groups made by one-way ANOVA ($P < 0.0001$; significance comparisons: * vs. vector control; † vs. vector control plus LPS; and ‡ vs. Elk-3 overexpression in the absence of LPS). (B) Bone marrow-derived macrophages were isolated and cultured from WT and HO-1 KO mice, as described in Materials and Methods. GFP-labeled *E. coli* was added at 10 MOI/cell to the macrophages. After 2 h, cells were washed and processed for phagocytosis, as described. (Left and middle) Representative flow cytometry zebra plots for macrophages (F4/80+), WT or HO-1 KO, which phagocytized GFP-labeled *E. coli*. Quantification is assessed by MFI. (Right) The data are presented as percentage MFI of WT cells, $n = 3$ independent experiments, with testing by unpaired *t*-test (*$P = 0.0014$, significance comparison vs. WT). (C) RAW 264.7 were transfected with pFLAG-CMV-5a-HO-1 or vector control. GFP-labeled *E. coli* was added at 10 MOI/cell. After 2 h, cells were washed and processed for phagocytosis, as described in Materials and Methods. (Left and middle) Representative flow cytometry zebra plots for macrophages (F4/80+), transfected with vector control or HO-1, which phagocytized GFP-labeled *E. coli*. Quantification is assessed by MFI. (Right) The data are presented as percentage MFI of vector control, $n = 12$ (4 independent experiments), with testing by unpaired *t*-test (*$P = 0.021$, significance comparison vs. vector control).

overexpression of the activator Sp1 resulted in an increase in Elk-3 promoter activity. ChIP analysis demonstrated that stimulation of mouse macrophages with LPS resulted in an increased binding of KLF4 to the Elk-3 promoter at the GC-rich binding site from −613 to −603 (Fig. 5C). In contrast, during LPS stimulation, the binding of Sp1 in this same region is decreased (Fig. 5C). Taken together, these data suggest that KLF4 promotes a decrease in Elk-3 promoter activity by directly binding to the Elk-3 promoter and also by decreasing binding of the activator Sp1. Finally, the silencing of endogenous KLF4 in macrophages led to an attenuated reduction in Elk-3 promoter activity by LPS (Fig. 5D), confirming its importance in the down-regulation of Elk-3 by LPS.

KLF4 is expressed in mouse macrophages, and its expression is markedly increased by proinflammatory mediators, including LPS [41]. Additional studies showed that KLF4 contributes to the regulation of signaling pathways that control activation of macrophages. Moreover, investigations in KLF4-deficient mice have shown that KLF4 is essential for the differentiation of monocytes [42]. These studies support KLF4 and the genes targeted by KLF4 as crucial for macrophage biology.

Beyond gene regulation, we also wanted to understand the role of Elk-3 in the function of macrophages. Previously, Park and colleagues [43] demonstrated that stabilin-1, an Ets-2-regulated gene, promotes phagocytosis of apoptotic cells by macrophages in an acidic environment. Moreover, the ETS family member PU.1 is important for neutrophil function, and an absence of PU.1 results in ineffective bacterial uptake and killing [44]. With the consideration of these properties of other ETS proteins, we decided to investigate the role of Elk-3 in macrophage phagocytosis of bacteria. Elk-3 was overexpressed in RAW 264.7 cells and then exposed to *E. coli* bacteria. Assessment of the cells by confocal microscopy showed that overexpression of Elk-3 led to a marked reduction in the percentage of macrophages phagocytizing bacteria (Fig. 6B) compared with control cells, and overall, there was a significant decrease in the amount of phagocytized, GFP-labeled *E. coli* in macrophages overexpressing Elk-3 (Fig. 6C). On the contrary, the silencing of Elk-3 in RAW 264.7 cells resulted in an acute increase in the phagocytosis of *E. coli* (Fig. 6D).

In the presence of *E. coli* LPS, transfection of the Elk-3 transgene resulted in an expression level of Elk-3 comparable

with basal levels (Fig. 6A), which subsequently resulted in a blunted induction of HO-1 protein in macrophages (Fig. 7A). Thus, we next assessed the ability of primary bone marrow-derived macrophages, harvested from HO-1 KO mice, to phagocytize *E. coli* bacteria. Figure 7B reveals that a deficiency in HO-1 protein resulted in a 50% decrease in phagocytosis of *E. coli* by macrophages, which is similar to the reduction in phagocytosis by macrophages overexpressing Elk-3 (Fig. 6C). Moreover, overexpression of HO-1 protein in macrophages resulted in an increased phagocytosis of *E. coli* by the cells (Fig. 7C). These data suggest that the down-regulation of Elk-3 in an activated macrophage during exposure to bacteria contributes to the ability of macrophages to phagocytize bacteria, in part, by increased expression of HO-1.

We have demonstrated previously that transgenic overexpression of HO-1 in mice leads to increased peritoneal phagocytosis of bacteria in vivo [24]. Moreover, the downstream product of heme catabolism by HO-1, carbon monoxide, is also able to increase bacterial phagocytosis by immune cells in vivo [24], and macrophages exposed to carbon monoxide have an improved ability to phagocytize apoptotic cells and accelerate the resolution of inflammation during a systemic response in mice [45]. Thus, we propose that the down-regulation of Elk-3 during exposure to bacteria (or their associated endotoxin), in part, driven by the transcriptional repressor KLF4, allows for up-regulation of HO-1 and a compensatory response to clear bacteria and then resolve the inflammatory response.

AUTHORSHIP

K.T. offered the conception and design, collection and/or assembly of data, data analysis and interpretation, and manuscript writing. A.M.G., H.C., X.L., and S.W.C. provided the conception and design and data analysis and interpretation. M.A.P. offered the conception and design, data analysis and interpretation, manuscript writing, and final approval of the manuscript.

ACKNOWLEDGMENTS

DISCLOSURES

The authors declare no conflict of interest.

REFERENCES

1. Charlot, C., Dubois-Pot, H., Serchov, T., Tourrette, Y., Wasylyk, B. (2010) A review of post-translational modifications and subcellular localization of Ets transcription factors: possible connection with cancer and involvement in the hypoxic response. *Methods Mol. Biol.* **647,** 3–30.
2. Oikawa, T., Yamada, T. (2003) Molecular biology of the Ets family of transcription factors. *Gene* **303,** 11–34.
3. Dittmer, J., Nordheim, A. (1998) Ets transcription factors and human disease. *Biochim. Biophys. Acta* **1377,** F1–F11.
4. Garrett-Sinha, L. A. (2013) Review of Ets1 structure, function, and roles in immunity. *Cell. Mol. Life Sci.* **70,** 3375–3390.
5. Buchwalter, G., Gross, C., Wasylyk, B. (2004) Ets ternary complex transcription factors. *Gene* **324,** 1–14.
6. Lopez, M., Oettgen, P., Akbarali, Y., Dendorfer, U., Libermann, T. A. (1994) ERP, a new member of the ets transcription factor/oncoprotein family: cloning, characterization, and differential expression during B-lymphocyte development. *Mol. Cell. Biol.* **14,** 3292–3309.
7. Giovane, A., Pintzas, A., Maira, S. M., Sobieszczuk, P., Wasylyk, B. (1994) Net, a new ets transcription factor that is activated by Ras. *Genes Dev.* **8,** 1502–1513.
8. Maira, S. M., Wurtz, J. M., Wasylyk, B. (1996) Net (ERP/SAP2) one of the Ras-inducible TCFs, has a novel inhibitory domain with resemblance to the helix-loop-helix motif. *EMBO J.* **15,** 5849–5865.
9. Criqui-Filipe, P., Ducret, C., Maira, S. M., Wasylyk, B. (1999) Net, a negative Ras-switchable TCF, contains a second inhibition domain, the CID, that mediates repression through interactions with CtBP and de-acetylation. *EMBO J.* **18,** 3392–3403.
10. Giovane, A., Sobieszczuk, P., Ayadi, A., Maira, S. M., Wasylyk, B. (1997) Net-b, a Ras-insensitive factor that forms ternary complexes with serum response factor on the serum response element of the fos promoter. *Mol. Cell. Biol.* **17,** 5667–5678.
11. Kerr, N., Pintzas, A., Holmes, F., Hobson, S. A., Pope, R., Wallace, M., Wasylyk, C., Wasylyk, B., Wynick, D. (2010) The expression of ELK transcription factors in adult DRG: novel isoforms, antisense transcripts and upregulation by nerve damage. *Mol. Cell. Neurosci.* **44,** 165–177.
12. Chen, Y.-H., Layne, M. D., Chung, S. W., Ejima, K., Baron, R. M., Yet, S.-F., Perrella, M. A. (2003) Elk-3 is a transcriptional repressor of nitric-oxide synthase 2. *J. Biol. Chem.* **278,** 39572–39577.
13. Chung, S. W., Chen, Y.-H., Yet, S.-F., Layne, M. D., Perrella, M. A. (2006) Endotoxin-induced down-regulation of Elk-3 facilitates heme oxygenase-1 induction in macrophages. *J. Immunol.* **176,** 2414–2420.
14. Chung, S. W., Chen, Y. H., Perrella, M. A. (2005) Role of Ets-2 in the regulation of heme oxygenase-1 by endotoxin. *J. Biol. Chem.* **280,** 4578–4584.
15. Chung, S. W., Kwon, M. Y., Kang, Y. H., Chung, H. T., Lee, S. J., Kim, H. P., Perrella, M. A. (2012) Transforming growth factor-β1 suppression of endotoxin-induced heme oxygenase-1 in macrophages involves activation of Smad2 and downregulation of Ets-2. *J. Cell. Physiol.* **227,** 351–360.
16. Hung, C. C., Liu, X., Kwon, M. Y., Kang, Y. H., Chung, S. W., Perrella, M. A. (2010) Regulation of heme oxygenase-1 gene by peptidoglycan involves the interaction of Elk-1 and C/EBPalpha to increase expression. *Am. J. Physiol. Lung Cell. Mol. Physiol.* **298,** L870–L879.
17. Wiesel, P., Foster, L. C., Pellacani, A., Layne, M. D., Hsieh, C.-M., Huggins, G. S., Strauss, P., Yet, S.-F., Perrella, M. A. (2000) Thioredoxin facilitates the induction of heme oxygenase-1 in response to inflammatory mediators. *J. Biol. Chem.* **275,** 24840–24846.
18. Alam, J., Cook, J. L. (2007) How many transcription factors does it take to turn on the heme oxygenase-1 gene? *Am. J. Respir. Cell Mol. Biol.* **36,** 166–174.
19. Abraham, N. G., Kappas, A. (2005) Heme oxygenase and the cardiovascular-renal system. *Free Radic. Biol. Med.* **39,** 1–25.
20. Maines, M. D., Gibbs, P. E. M. (2005) 30 Some years of heme oxygenase: from a "molecular wrecking ball" to a "mesmerizing" trigger of cellular events. *Biochem. Biophys. Res. Commun.* **338,** 568–577.
21. Ryter, S. W., Alam, J., Choi, A. M. K. (2006) Heme oxygenase-1/carbon monoxide: from basic science to therapeutic applications. *Physiol. Rev.* **86,** 583–650.
22. Ryter, S. W., Otterbein, L. E., Morse, D., Choi, A. M. K. (2002) Heme oxygenase/carbon monoxide signaling pathways: regulation and functional significance. *Mol. Cell. Biochem.* **234–235,** 249–263.
23. Wiesel, P., Patel, A. P., DiFonzo, N., Marria, P. B., Sim, C. U., Pellacani, A., Maemura, K., LeBlanc, B. W., Marino, K., Doerschuk, C. M., Yet, S. F., Lee, M. E., Perrella, M. A. (2000) Endotoxin-induced mortality is related to increased oxidative stress and end-organ dysfunction, not refractory hypotension, in heme oxygenase-1-deficient mice. *Circulation* **102,** 3015–3022.
24. Chung, S. W., Liu, X., Macias, A. A., Baron, R. M., Perrella, M. A. (2008) Heme oxygenase-1-derived carbon monoxide enhances the host defense response to microbial sepsis in mice. *J. Clin. Invest.* **118,** 239–247.
25. Tsoyi, K., Lee, T. Y., Lee, Y. S., Kim, H. J., Seo, H. G., Lee, J. H., Chang, K. C. (2009) Heme-oxygenase-1 induction and carbon monoxide-releasing molecule inhibit lipopolysaccharide (LPS)-induced high-mobility group box 1 release in vitro and improve survival of mice in

LPS- and cecal ligation and puncture-induced sepsis model in vivo. *Mol. Pharmacol.* **76,** 173–182.

26. Minamino, T., Christou, H., Hsieh, C.-M., Liu, Y., Dhawan, V., Abraham, N. G., Perrella, M. A., Mitsialis, S. A., Kourembanas, S. (2001) Targeted expression of heme oxygenase-1 prevents the pulmonary inflammatory and vascular responses to hypoxia. *Proc. Natl. Acad. Sci. USA* **98,** 8798–8803.

27. Gross, C., Buchwalter, G., Dubois-Pot, H., Cler, E., Zheng, H., Wasylyk, B. (2007) The ternary complex factor net is downregulated by hypoxia and regulates hypoxia-responsive genes. *Mol. Cell. Biol.* **27,** 4133–4141.

28. Gross, C., Dubois-Pot, H., Wasylyk, B. (2008) The ternary complex factor Net/Elk-3 participates in the transcriptional response to hypoxia and regulates HIF-1 alpha. *Oncogene* **27,** 1333–1341.

29. Yet, S.-F., Perrella, M. A., Layne, M. D., Hsieh, C.-M., Maemura, K., Kobzik, L., Wiesel, P., Christou, H., Kourembanas, S., Lee, M.-E. (1999) Hypoxia induces severe right ventricular dilatation and infarction in heme oxygenase-1 null mice. *J. Clin. Invest.* **103,** R23–R29.

30. Ejima, K., Layne, M. D., Carvajal, I. M., Nanri, H., Ith, B., Yet, S.-F., Perrella, M. A. (2002) Modulation of the thioredoxin system during inflammatory responses and its effect on heme oxygenase-1 expression. *Antioxid. Redox Signal.* **4,** 569–575.

31. Nakahira, K., Haspel, J. A., Rathinam, V. A., Lee, S. J., Dolinay, T., Lam, H. C., Englert, J. A., Rabinovitch, M., Cernadas, M., Kim, H. P., Fitzgerald, K. A., Ryter, S. W., Choi, A. M. (2011) Autophagy proteins regulate innate immune responses by inhibiting the release of mitochondrial DNA mediated by the NALP3 inflammasome. *Nat. Immunol.* **12,** 222–230.

32. Schmittgen, T. D., Livak, K. J. (2008) Analyzing real-time PCR data by the comparative C(T) method. *Nat. Protoc.* **3,** 1101–1108.

33. Kwon, M. Y., Liu, X., Lee, S. J., Kang, Y. H., Choi, A. M., Lee, K. U., Perrella, M. A., Chung, S. W. (2011) Nucleotide-binding oligomerization domain protein 2 deficiency enhances neointimal formation in response to vascular injury. *Arterioscler. Thromb. Vasc. Biol.* **31,** 2441–2447.

34. Zhou, X., Qiu, W., Sathirapongsasuti, J. F., Cho, M. H., Mancini, J. D., Lao, T., Thibault, D. M., Litonjua, A. A., Bakke, P. S., Gulsvik, A., Lomas, D. A., Beaty, T. H., Hersh, C. P., Anderson, C., Geigenmuller, U., Raby, B. A., Rennard, S. I., Perrella, M. A., Choi, A. M., Quackenbush, J., Silverman, E. K. (2013) Gene expression analysis uncovers novel hedgehog interacting protein (HHIP) effects in human bronchial epithelial cells. *Genomics* **101,** 263–272.

35. Hall, S. R., Tsoyi, K., Ith, B., Padera Jr., R. F., Lederer, J. A., Wang, Z., Liu, X., Perrella, M. A. (2013) Mesenchymal stromal cells improve survival during sepsis in the absence of heme oxygenase-1: the importance of neutrophils. *Stem Cells* **31,** 397–407.

36. Kaczynski, J., Cook, T., Urrutia, R. (2003) Sp1- and Krüppel-like transcription factors. *Genome Biol.* **4,** 206.

37. Lomberk, G., Urrutia, R. (2005) The family feud: turning off Sp1 by Sp1-like KLF proteins. *Biochem. J.* **392,** 1–11.

38. Silva, M. T. (2010) When two is better than one: macrophages and neutrophils work in concert in innate immunity as complementary and cooperative partners of a myeloid phagocyte system. *J. Leukoc. Biol.* **87,** 93–106.

39. Ai, W., Liu, Y., Langlois, M., Wang, T. C. (2004) Kruppel-like factor 4 (KLF4) represses histidine decarboxylase gene expression through an upstream Sp1 site and downstream gastrin responsive elements. *J. Biol. Chem.* **279,** 8684–8693.

40. Shie, J. L., Chen, Z. Y., Fu, M., Pestell, R. G., Tseng, C. C. (2000) Gut-enriched Krüppel-like factor represses cyclin D1 promoter activity through Sp1 motif. *Nucleic Acids Res.* **28,** 2969–2976.

41. Feinberg, M. W., Cao, Z., Wara, A. K., Lebedeva, M. A., Senbanerjee, S., Jain, M. K. (2005) Kruppel-like factor 4 is a mediator of proinflammatory signaling in macrophages. *J. Biol. Chem.* **280,** 38247–38258.

42. Alder, J. K., Georgantas III, R. W., Hildreth, R. L., Kaplan, I. M., Morisot, S., Yu, X., McDevitt, M., Civin, C. I. (2008) Kruppel-like factor 4 is essential for inflammatory monocyte differentiation in vivo. *J. Immunol.* **180,** 5645–5652.

43. Park, S. Y., Bae, D. J., Kim, M. J., Piao, M. L., Kim, I. S. (2012) Extracellular low pH modulates phosphatidylserine-dependent phagocytosis in macrophages by increasing stabilin-1 expression. *J. Biol. Chem.* **287,** 11261–11271.

44. Anderson, K. L., Smith, K. A., Pio, F., Torbett, B. E., Maki, R. A. (1998) Neutrophils deficient in PU.1 do not terminally differentiate or become functionally competent. *Blood* **92,** 1576–1585.

45. Chiang, N., Shinohara, M., Dalli, J., Mirakaj, V., Kibi, M., Choi, A. M., Serhan, C. N. (2013) Inhaled carbon monoxide accelerates resolution of inflammation via unique proresolving mediator-heme oxygenase-1 circuits. *J. Immunol.* **190,** 6378–6388.